International Journal of Earth, Energy and Environmental Sciences
ISSN: 2517-942X
Vol:9, No:7, 2015

Durability Enhancement of $CaSO_4$ in Repetitive Operation of Chemical Heat Pump

Y. Shiren, M. Masuzawa, H. Ohkura, T. Yamagata, Y. Aman, N. Kobayashi

***Abstract*—**An important problem for the $CaSO_4/CaSO_4 \cdot 1/2H_2O$ Chemical heat pump (CHP) is that the material is deactivated through repetitive reaction between hydration and dehydration in which the crystal phase of the material is transformed from III-$CaSO_4$ to II-$CaSO_4$. We investigated suppression on the phase change by adding a sulfated compound. The most effective material was $MgSO_4$. $MgSO_4$ doping increased the durability of $CaSO_4$ in the actual CHP repetitive cycle of hydration/dehydration to 3.6 times that of undoped $CaSO_4$. The $MgSO_4$-doped $CaSO_4$ showed a higher phase transition temperature and activation energy for crystal transformation from III-$CaSO_4$ to II-$CaSO_4$. $MgSO_4$ doping decreased the crystal lattice size of $CaSO_4 \cdot 1/2H_2O$ and II-$CaSO_4$ to smaller than that of undoped $CaSO_4$. Modification of the crystal structure is considered to be related to the durability change in $CaSO_4$ resulting from $MgSO_4$ doping.

***Keywords*—**$CaSO_4$, chemical heat pump, durability of chemical heat storage material, heat storage.

I. Introduction

IN recent years, we have recognized the need to deal with environmental problems and energy depletion. Of the primary energy consumed in Japan, 45% is discarded as waste heat [1]. Regarding the exhaust heat from industry, 70% of the waste heat is below 200°C [2]. Low-temperature waste heat can be used as a countermeasure to the environmental and energy problem. Expectations are that chemical heat pumps (CHPs) can run on waste heat.

CHP is a heat pump system that uses reversible exothermic reaction, mainly between the chemical heat storage material and condensable gases. In operation, CHP has three modes: the temperature-increasing mode, in which high temperature heat is obtained using middle temperature waste heat; the heat-enhance mode, in which inputting high temperature waste heat and environmental heat to CHP makes more middle heat output than the input of high temperature heat; and the cooling mode in which CHP generates cold heat from high or middle temperature waste heat.

We can choose chemical heat storage materials for the CHP system, of which the $CaSO_4/CaSO_4 \cdot 1/2H_2O$ CHP system that uses a vapor-solid reaction of (1) is suitable for low-temperature waste heat.

$$III - CaSO_4 + 1/2H_2O(g) = \beta - CaSO_4 \cdot 1/2H_2O + 32.886\ kJ/mol \quad (1)$$

Y. Shiren, M. Masuzawa, H. Ohkura, T. Yamagata, and Y. Aman are with the Ricoh Institute of Technology, Ricoh ltd., Japan (phone: +81-50-3817-4895 e-mail: yohhei.shren@ nts.ricoh.co.jp).

N. Kobayashi is with the Chemical and Biological Engineering Department, Nagoya University, Japan, (e-mail: kobayashi@energy.gr.jp).

This system can generate about 180°C heat in temperature-increasing mode or about 5°C heat in the cooling mode from waste heat of around 130°C. Further, this system has the advantages that gypsum is inexpensive, the system uses no toxicants, and it is easy to design the reactor vessel because the change in volume of the $CaSO_4$ is small between the III-$CaSO_4$ and β-$CaSO_4 \cdot 1/2H_2O$.

We must overcome deactivation of the $CaSO_4$ through repetitive reaction to put the $CaSO_4/CaSO_4 \cdot 1/2H_2O$ CHP system into practical use. This is needed because the output of the CHP decreases with the deactivation. The deactivation of $CaSO_4$ is a change in crystal structure from III-$CaSO_4$ to II-$CaSO_4$. II-$CaSO_4$ does not react with water vapor and it is difficult to regenerate it to III-$CaSO_4$. For that reason, the phase change to II-$CaSO_4$ should be avoided.

The highest reaction temperature of the $CaSO_4/CaSO_4 \cdot 1/2H_2O$ CHP system, which is 191°C when the system is run under 101.3kPa water vapor, is lower than 250°C, the temperature at which III-$CaSO_4$ starts to change to II-$CaSO_4$ in dry air [3]. However, Gardet et al. showed that the phase change temperature to II-$CaSO_4$ decreases in water vapor [4]; in CHP operation, Lee et al. also reported a phase change to II-$CaSO_4$ [5]. The II-$CaSO_4$ phase change is enhanced at higher temperature and water vapor pressure posing a serious problem, especially in the temperature-increasing mode.

When we took into account that the inertness of II-$CaSO_4$ comes from stability of the crystal structure, we expected that lattice distortion of the $CaSO_4$ that results from substituting other atoms for Ca-cites would inhibit the phase change resulting from stabilization of III-$CaSO_4$ or destabilization of II-$CaSO_4$.

In this study, we investigated suppression on the phase change from III-$CaSO_4$ to II-$CaSO_4$ by adding a sulfated compound based on that expectation. The purpose was to inhibit the reduction of heat output in the CHP operation.

II. Experiment

First, the most effective additive for the phase change inhibition to II-CaSO4 was examined using various sulfated compounds by screening experiments. $MgSO_4$ was then added to $CaSO_4$, which was best in the screening experiments; this was examined by repeating the hydration/dehydration cycle to confirm suppression with the additive on phase change to II-$CaSO_4$ in the CHP operation. We also investigated the changes of thermal property and crystal structure when $MgSO_4$ is added.

A. Screening Experiment

1. Specimen Preparation

Aqueous solutions were prepared for mixing with β-$CaSO_4 \cdot 1/2H_2O$ so that the additive amount of 0.5, 1.0, 5.0mol% per 1mol of β-$CaSO_4 \cdot 1/2H_2O$ was mixed with water; water weight was at 74% of β-$CaSO_4 \cdot 1/2H_2O$. Tried additive was $MgSO_4 \cdot 7H_2O$, K_2SO_4, Na_2SO_4, $FeSO_4 \cdot 7H_2O$, $AlK(SO_4)_2 \cdot 12H_2O$, and $AlNa(SO_4)_2 \cdot 12H_2O$. The aqueous solution and β-$CaSO_4 \cdot 1/2H_2O$ powder was mixed and stirred, and then casted into a silicone-mold of 25mm × 25mm × 5mm and cured. The samples were dehydrated by heating at 150°C for 5hrs in a vacuum and stored in a laboratory environment. In the laboratory environment, $CaSO_4$ was fully hemihydrated by reacting with water vapor in the atmosphere.

2. Batch Process to Turn into II-$CaSO_4$

Fig. 1 shows the experimental apparatus for turning into II-$CaSO_4$ by heating in water vapor in a batch process.

The sample cell holding the sample and the evaporator half filled by water are connected via pipes and valve V1. Constant water vapor pressure is applied to the sample by opening valve V1. Temperature of the sample cell was kept at 180°C and that of the evaporator was at 100°C; pressure of the water vapor was 101.3kPa. The piping section was heated to 120°C by the heater to prevent condensation of the vapor.

Samples were set on the sample holder and placed in the sample cell preheated to 180°C and evacuated for 30 min. In that time the samples were dehydrated from hemihydrate gypsum. After evacuation, valve V3 was closed. The samples were exposed to 101.3kPa water vapor by opening valve V1 for 150 min. The samples were dehydrated by evacuating for 15 min after closing valve V1 and opening valve V3. The samples were kept in the laboratory environment for more than one day.

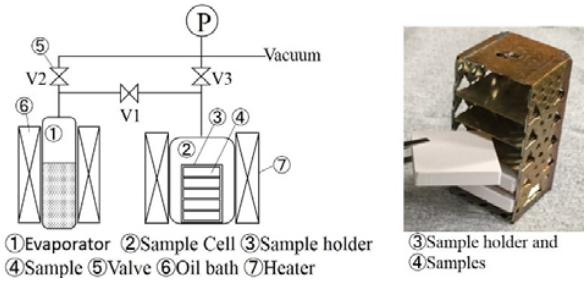

Fig. 1 Setup of screening experiment

The II-$CaSO_4$ rate was measured using X-ray diffraction. As the crystal structure of II-$CaSO_4$ and $CaSO_4 \cdot 1/2H_2O$, which was hydrated from III-$CaSO_4$ in the laboratory environment, is different, the diffraction profile obtained by the X-ray diffraction measurement is also different. Therefore, the diffraction profile of the sample, which includes both crystal types, is obtained in the form of overlapping individual peaks. Because there is correlation between the mixture ratio of the crystal phases and the peak strength ratio of both phases, the mixture ratio of II-$CaSO_4$ in an unknown sample is estimated by measuring the peak strength ratio of a known sample. Peaks for estimating the mixture ratio were selected that do not overlap peaks of the $CaSO_4 \cdot 1/2H_2O$ and II-$CaSO_4$; i.e., the intensities of the peak areas at $2\theta = 29.9^o$ for $CaSO_4 \cdot 1/2H_2O$ and at $2\theta = 36.4^o$ for II-$CaSO_4$ were compared in the condition that diffracted X-ray wavelength is $\lambda = 1.54006$Å.

B. Hydration/dehydration Cycle Experiment

1. Specimen Preparation

The $CaSO_4$ samples mixed with 0, 2, 4mol% of $MgSO_4$ were made in the same way as II-A(1) except that α-$CaSO_4 \cdot 1/2H_2O$ was used instead of β-$CaSO_4 \cdot 1/2H_2O$; mixed water was 40% of α-$CaSO_4 \cdot 1/2H_2O$; and thickness of the sample was 1mm instead of 5mm to finish hydration/dehydration in the cycle experiment.

2. Experiment Apparatus

Fig. 2 shows the experimental apparatus. The sample was placed on the heat flux sensor in the sample cell and the hydration/dehydration cycle experiment was operated in the experimental program controlling water vapor pressure. Constant flow of water vapor was supplied to the sample cell through the mass flow controller, and the water vapor pressure applied to the sample was kept constant by controlling the outflow using the control valve. The amount of hydration and dehydration of the sample was measured in units of seconds from the difference in steam flow between the mass flow controller and the mass flow meter. Also, the amount of heat input and output to the sample was measured in units of seconds from the heat flux sensor underneath the sample.

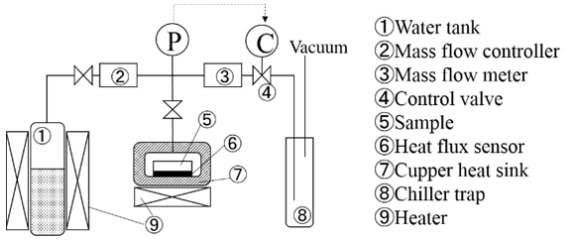

Fig. 2 Experiment equipment for Hydration/dehydration cycle experiment

In this experiment, the increasing ratio of II-$CaSO_4$ through the hydration/dehydration cycles is estimated from the decrease in heat output measured by the heat flux sensor. As only III-$CaSO_4$ reacts with water vapor, the ratio of II-$CaSO_4$ at each cycle is obtained by measuring the decreasing ratio of the output heat at the time compared to the initial output heat.

3. Experiment Conditions

Hydration and dehydration cycles were repeated under the conditions that temperature of the sample cell was kept at 150°C and the steam pressure of 100kPa or 3.2kPa was added to the sample alternately at 10min intervals. Undoped $CaSO_4$ underwent 100 cycles and $MgSO_4$-2, 4mol%-doped $CaSO_4$ underwent 400 cycles.

C. PHYSICAL Properties Analysis of $MgSO_4$-doped $CaSO_4$

1. Thermal Analysis

TG-DTA analysis of $MgSO_4$-2, 4mol%-doped and undoped $CaSO_4$ samples, which did not undergo the de/hydration cycle experiment, was performed to measure the phase transition temperature from III-$CaSO_4$ to II-$CaSO_4$ in dry air.

The activation energies to II-$CaSO_4$ were estimated by Kissinger relation for the same samples with the TG-DTA measurement. Estimation was made using DTA measurement, in which the rate of temperature rise was varied at 6, 10, and 20°C/min.

The Kissinger relation represents the relationship between activation energy E and the variety of DTA peak temperature T_m with the rate of temperature rise φ of DTA measurement in exoergic or endoergic reaction [6], [7]. The Kissinger relation is

$$E R^{-1} T_m^{-1} = -\ln\left(\phi \mathrm{R}^{-1} T_m^{-2}\right) + \ln(\mathrm{EA}^{-1}) \quad (2)$$

where R is gas constant and A is frequency factor.

2. Analysis of Crystal Structure

Synchrotron radiation X-ray diffraction measurement was performed to investigate the change in crystalline structure of the $CaSO_4$. This was done by mixing $MgSO_4$ before and after the hydration/dehydration cycle experiment and the mixed states of $MgSO_4$ in the samples.

$MgSO_4$-1, 2, 4mol%-doped and undoped $CaSO_4$ samples were measured by XRD; these were made in the manner of II-B-1 and de/hydrated 0, 100, 390 times in the experiment of II-B-3. Before XRD measurement, the samples were stored in laboratory conditions where $CaSO_4$ and $MgSO_4$ were each hydrated to $CaSO_4 \cdot 1/2H_2O$ and $MgSO_4 \cdot 6H_2O$.

III. Results

A. Screening Experiment Results

Fig. 3 shows the screening experiment results. Suppression to II-$CaSO_4$ is shown in the samples adding $MgSO_4$, K_2SO_4, $FeSO_4$, and $AlK(SO_4)_2$. $MgSO_4$ achieved the best suppression. The accelerative effect to II-$CaSO_4$ is shown in the samples adding Na_2SO_4 and $AlNa(SO_4)_2$.

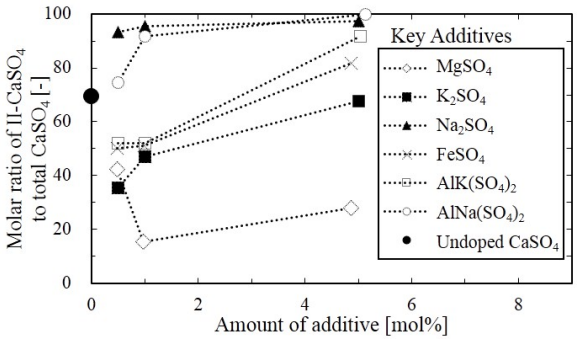

Fig. 3 Molar ratio of II-$CaSO_4$ to total $CaSO_4$ in the $CaSO_4$ samples mixed with sulfated compounds after the batch process to turn into II-$CaSO_4$

B. Results of the Hydration/dehydration Cycle Experiment of $MgSO_4$-doped $CaSO_4$

Fig. 4 shows the results of the hydration/dehydration cycle experiment of $MgSO_4$-doped $CaSO_4$. The rate of output decline of $MgSO_4$-doped $CaSO_4$ was slower than that of undoped $CaSO_4$, which means that adding $MgSO_4$ in $CaSO_4$ is effective in suppressing III-$CaSO_4$ to II-$CaSO_4$ in the CHP operation. By adding $MgSO_4$, the CHP cycle operation number until a 20% decline in the output increased to 112 times from 31 times of the undoped $CaSO_4$ – extended about 3.6 times. There were few differences in suppression between 2mol% and 4mol% of $MgSO_4$ doping.

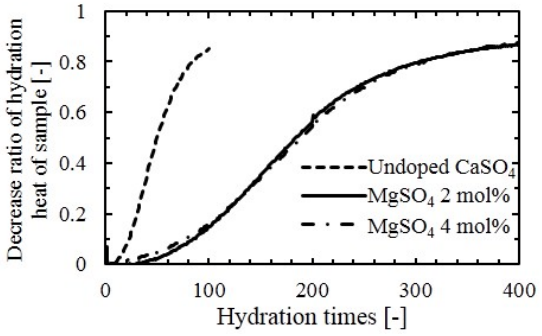

Fig. 4 Decrease ratio of hydration heat output of $CaSO_4$ samples mixed with 0, 2, 4mol% of $MgSO_4$ to initial hydration heat output of each samples in hydration/dehydration cycle experiment

Table I shows the hemihydration heat of each sample in the third hydration of the cycle experiment. The hydration heat measured by the heat flux sensor is standardized by the hydration amount of 1/2 mol as the hemihydration heat of the samples to compare the experimental values to the theoretical hemihydration heat of $CaSO_4$. The difference in hemihydration heat between the $MgSO_4$-doped and the undoped $CaSO_4$ was small, within ±2%, but the quantity of hydration per 1g of dried sample decreased. Total hydration heat per weight decreased by around 10% with the addition of $MgSO_4$.

TABLE I
Quantity and Heat of Hydration at 3rd Hydration in De/hydration Cycle Experiment

	n (*) [-]	Hydration heat [kJ/(1/2mol-H_2O)]
Undoped $CaSO_4$	1.05	30.19
$MgSO_4$_2mol%	0.95	29.63
$MgSO_4$_4mol%	0.94	30.76
Ideal $CaSO_4$	1	32.886

(*) n: Number that is standardized quantity of hydration per 1g of dried sample with quantity of ideal hemihydration of $CaSO_4$ of 1g

C. Results of Physical Properties Analysis

1. Result of Thermal Analysis

Fig. 5 shows the results of TG-DTA measurement of the transition temperature to II-$CaSO_4$ from III-$CaSO_4$ in dry air. TG profiles in Fig. 5 show that there is no weight change in the temperature region above 350°C. It means that the DTA peaks

above the temperature are not originated to dehydration from either $MgSO_4 \cdot nH_2O$ or $CaSO_4 \cdot nH_2O$; DTA peaks above 350°C indicate the phase transition from III-CaSO4 to II-CaSO4. DTA peaks of $MgSO_4$-2,4mol%-doped $CaSO_4$ shifted higher to 408, 415°C from 340°C of undoped $CaSO_4$.

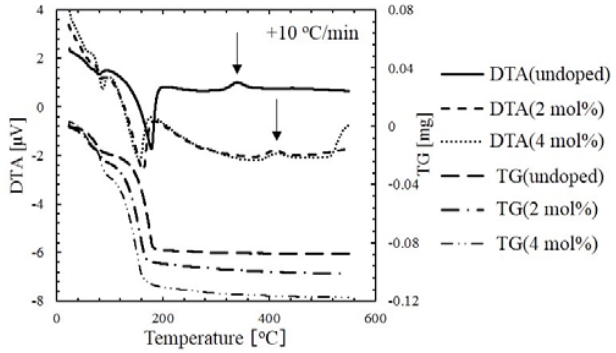

Fig. 5 Results of TG-DTA measurement of $CaSO_4$ samples mixed with 0, 2, 4mol% of $MgSO_4$

Table II shows the activation energy from III-$CaSO_4$ to II-$CaSO_4$ in dry air calculated by (2). $MgSO_4$-doped $CaSO_4$ had higher activation energy than undoped $CaSO_4$ from III-$CaSO_4$ to II-$CaSO_4$.

TABLE II
ACTIVATION ENERGY E ESTIMATED BY KISSINGER RELATION

	E [kJ/mol]
Undoped $CaSO_4$	168
$MgSO_4$ 2mol%	220
$MgSO_4$ 4mol%	229

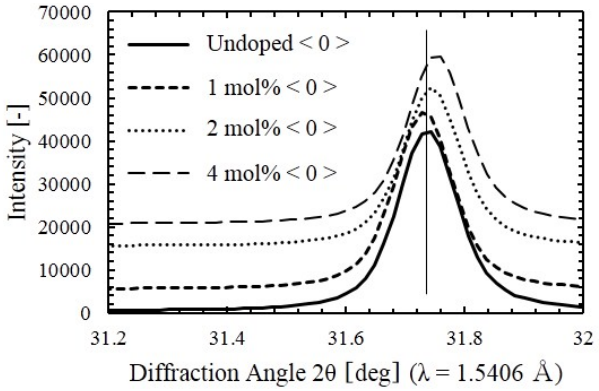

Fig. 6 XRD peak shift of $MgSO_4$-doped $CaSO_4 \cdot 1/2H_2O$ samples before hydration/dehydration cycle experiment

2. Results of Crystal Structure Analysis

The basic crystalline form of $CaSO_4$ did not change with the presence or absence of added $MgSO_4$, whereas the shifts of XRD peaks originated to gypsum were observed in the $MgSO_4$-doped samples. Fig. 6 shows the shifts of XRD peaks around 2θ=31.7° originated to $CaSO_4 \cdot 1/2H2O$. When the amount of $MgSO_4$ was increased in the sample, the XRD peaks shifted to a large diffraction angle; i.e., the lattice number decreased.

Also, the XRD peaks that originate to II-$CaSO_4$ after the hydration/dehydration cycle experiment seem to shift in direction, which means the lattice number decreases when $MgSO_4$ is added. Fig. 7 shows the XRD peaks around 2θ=55.7° originated to II-$CaSO_4$ of undoped $CaSO_4$ <100cycles>, $MgSO_4$-4mol%-doped $CaSO_4$ <100cycles>, and $MgSO_4$-4mol%-doped $CaSO_4$ <390cycles>. The molar ratio of II-CaSO4 in these samples is >90%, 36.7%, and >90% each. The peak position of $MgSO_4$-doped $CaSO_4$ in a relationally low ratio of II-$CaSO_4$ is the same as that of undoped $CaSO_4$, which is almost II-$CaSO_4$. In contrast, that of MgSO4-doped $CaSO_4$, which is almost II-$CaSO_4$, has a slightly smaller lattice number than that of undoped $CaSO_4$, which is almost II-$CaSO_4$.

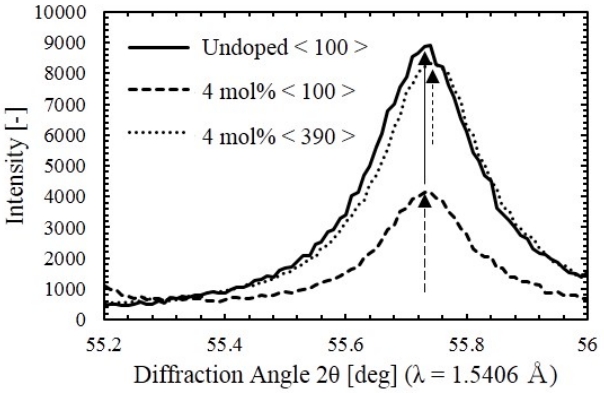

Fig. 7 Differences of XRD peaks of II-$CaSO_4$ between undoped and $MgSO_4$-4mol%-doped $CaSO_4$ after 100 and 390 cycles of hydration/dehydration

Fig. 8 shows the XRD profiles of the $MgSO_4$-doped and undoped samples before the hydration/dehydration experiment; the samples indicate the peaks of $MgSO_4 \cdot 6H_2O$ to be around 2θ=16.2, 17.3, 18.1°. The more $MgSO_4$ is added, the stronger the intensity of the $MgSO_4 \cdot 6H_2O$ peaks, which means the same amount of $MgSO_4$ remains in the sample as in a single compound.

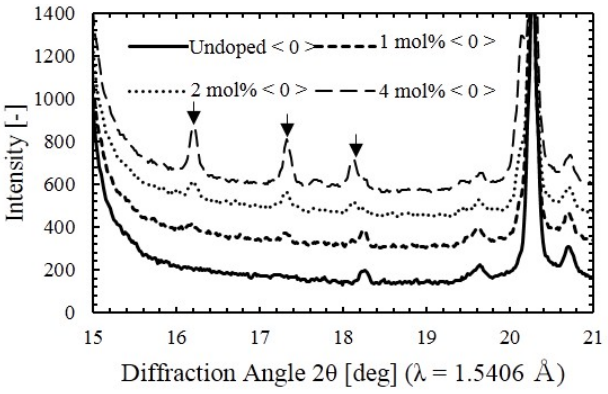

Fig. 8 Diffraction peaks originated to $MgSO_4 \cdot 6H_2O$ in XRD profile of $MgSO_4$-doped $CaSO_4 \cdot 1/2H_2O$ samples before hydration/dehydration cycle experiment

IV. Considerations

Considering the difference in suppression by adding sulfated compound to $CaSO_4$, the sulfated compounds constituted from Mg, which is the same group in the periodic table as Ca, K and Fe, which is the same row as Ca, are effective in suppressing deterioration to II-$CaSO_4$. In contrast, the sulfated compounds constituted from Na, which resides in a different group of the periodic table from Ca, accelerates the deterioration. These results lead us to infer that the sulfated compound constituted from the elements, which is easier to substitute to Ca sites of $CaSO_4$, indicates higher suppression. $MgSO_4$ indicated the highest suppression in the experiment. Because of that, the sulfated compounds constituted from Be, Zn, Sr, and Ba, which are in the same group of the periodic table as Ca and Mg, are suspected of suppressing deterioration to II-$CaSO_4$.

We next consider the relationship of suppression to II-$CaSO_4$, the activation energy to II-$CaSO_4$, and the changes in crystal structure.

Suppression to II-$CaSO_4$ of the $MgSO_4$-2mol% and 4mol%-doped sample is the same in the hydration/dehydration cycles experiment as shown in Fig. 4; the activation energies of these samples to II-$CaSO_4$ are approximately the same as shown in Table II. These results infer that an increase in the activation energy to II-$CaSO_4$ when $MgSO_4$ is added suppresses the phase change of III-$CaSO_4$ or $CaSO_4 \cdot 1/2H_2O$ to II-$CaSO_4$ in the hydration/dehydration cycles operation.

We then consider the change in lattice number when $MgSO_4$ is added. The lattice number of $CaSO_4 \cdot 1/2H_2O$ decreases when $MgSO_4$ is added before the cycle experiment, which infers that Mg atoms substitute Ca sites in specimen preparation. The decrease in lattice number may stem from the fact that the ionic radius of Mg^{2+} is smaller than that of Ca^{2+}. Beyond that, the lattice number of II-$CaSO_4$ also decreases at high II-$CaSO_4$ ratio as shown in Fig. 7, indicating that Mg atoms substitute Ca sites in II-$CaSO_4$ crystal, and the phase change to II-$CaSO_4$ starts from the part where $MgSO_4$ is well mixed next to the part where $MgSO_4$ is in low density or empty.

As described above, $MgSO_4$ is taken into the crystal of the $CaSO_4$ and changes the crystalline structure of $CaSO_4$. This is expected to suppress the phase change to II-$CaSO_4$.

It is therefore reasonable to assume that the activation energy to II-$CaSO_4$ increases with the change in crystalline structure of gypsum; i.e., as Mg atoms substituted to Ca sites inhibit the phase change from III-$CaSO_4$ to II-$CaSO_4$, higher energy is required for the phase change. However, rather than increasing Mg density, a threshold for a higher amount of Mg doping makes the crystal structure unstable, possibly promoting the phase transition to II-$CaSO_4$. This is supported by the supposition that high density of the sulfated compound promoted the phase change to II-$CaSO_4$ in the screening experiment.

V. Conclusion

This study discloses that adding $MgSO_4$ to $CaSO_4$ suppresses the phase change from III-$CaSO_4$ to II-$CaSO_4$ in operation of the CHP system. It also discloses that $MgSO_4$-doped $CaSO_4$ has a higher phase change temperature and activation energy from III-$CaSO_4$ to II-$CaSO_4$, and a lower lattice number than undoped $CaSO_4$.

A foothold in the technique to improve the durability of $CaSO_4$ in hydration/dehydration repetitive operation was found. This result will be an effective step in achieving temperature-increasing mode CHP utilizing $CaSO_4$.

References

[1] COCN, (Leading-edge technology to be applied to energy network), 2014, http://www.cocn.jp/common/pdf/thema63-L.pdf (accessed Jan 6th 2015)
[2] Energy Conservation Center, Japan, (Survey Research of factories waste heat), 2001, pp. 14.
[3] Society of Inorganic Materials, Japan ed., *Cement・Gypsum・Lime Handbook*, Giho-do, 1995, pp. 142-143.
[4] J. J. Gardet, B. Guilhot, M. Soustelle, Cement and Concrete Research. Vol. 6, 1976, pp. 193-200.
[5] Jun-Hee Lee, H. Ogura, S. Satoh, App. Term. Eng., Vol. 63, 1, Feb. 2014, pp. 192-199.
[6] H. E. Kissinger, Anal. Chem., Vol. 29, 11, pp. 1702-1706, 1957
[7] T. Kotoyori, "Energy of Activation for Oxidative Pyrolysis of Several Plastics", Research Report of the Research Institute of Industry Safety, RR-19-4. 1971, https://www.jniosh.go.jp/publication/doc/rr/RR-19-4.pdf (accessed Jan 6th 2015).